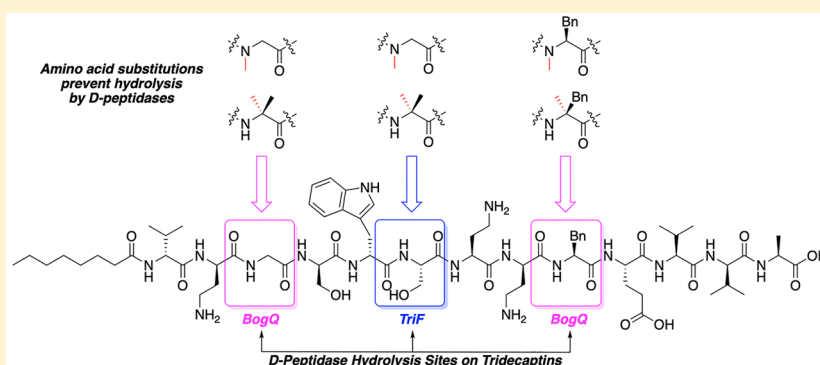


## A Chemical-Intervention Strategy To Circumvent Peptide Hydrolysis by D-Stereoselective Peptidases

Samantha J. Bann,<sup>†</sup> Ross D. Ballantine,<sup>†</sup> Conor E. McCallion,<sup>†</sup> Pei-Yuan Qian,<sup>‡</sup> Yong-Xin Li,<sup>§</sup> and Stephen A. Cochrane<sup>\*,†</sup><sup>†</sup>School of Chemistry and Chemical Engineering, Stranmillis Road, Queen's University Belfast, Belfast BT9 5AG, U.K.<sup>‡</sup>Department of Ocean Science, Division of Life Science and Hong Kong Branch of Southern Marine Science & Engineering Guangdong Laboratory, Hong Kong University of Science and Technology, Clear Water Bay, Hong Kong<sup>§</sup>Department of Chemistry, Hong Kong University, Hong Kong

## Supporting Information



**ABSTRACT:** D-Stereoselective peptidases that degrade nonribosomal peptides (NRPs) were recently discovered and could have serious implications for the future of NRPs as antibiotics. Herein, we report chemical modifications that can be used to impart resistance to the D-peptidases BogQ and TriF. New tridecaptin A analogues were synthesized that retain strong antimicrobial activity and have significantly enhanced D-peptidase stability. *In vitro* assays confirmed that synthetic analogues retain the ability to bind to their cellular receptor, peptidoglycan intermediate lipid II.

## INTRODUCTION

Nonribosomal peptides (NRPs) are a diverse class of natural products that are biosynthesized in bacteria and fungi by nonribosomal peptide synthetases (NRPSes).<sup>1,2</sup> As the synthesis of these peptides is not governed by the ribosome, a huge variety of nonproteinogenic amino acids are found in NRPs, many of which are also macrocyclic peptides. As well as providing a source of huge-structural variability among NRPs, these factors often impart superior stability to peptidases found in plasma and the GI tract.<sup>3</sup> This is because most peptidases are only capable of hydrolyzing peptide bonds composed of L-amino acids (i.e., ribosomally synthesized). It is therefore not surprising that NRPs hold a privileged position in antibiotic discovery and design.<sup>4–6</sup> In the golden era of antibiotics the large structural diversity of NRPs provided many different scaffolds for antibiotic lead compounds. This includes many antibiotics still in use today, such as penicillin, vancomycin, ramoplanin, polymyxin E (colistin), daptomycin, and bacitracin. With the rise of antimicrobial resistance, novel antimicrobial compounds are desperately needed. In recent years a plethora of NRPs that kill multidrug resistant (MDR) bacteria have been discovered or characterized.<sup>6</sup> This includes compounds that exclusively target MDR Gram-positive

bacteria, such as teixobactin,<sup>7</sup> lugdunin,<sup>8</sup> lysocin E,<sup>9</sup> and the humimycins,<sup>10</sup> as well as those that can kill MDR Gram-negatives, such as brevicidine and laterocidine<sup>11</sup> and tridecaptin A<sub>1</sub>.<sup>12</sup> These recently discovered NRPs and the aforementioned clinically approved NRPs all contain D-amino acids, making them highly resistant to most peptidases.

If bacteria produce an antimicrobial compound, they must have a self-protection mechanism to prevent them succumbing to its effects. The genetic determinants responsible for this intrinsic resistance are often found in the biosynthetic gene cluster (BGC) that encodes the enzymes that synthesize that antimicrobial compound.<sup>13</sup> These BGC-encoded resistance mechanisms are an emerging source of resistance that could be clinically relevant.<sup>14–16</sup> Recently, D-stereoselective peptidases that hydrolyze D-amino acid containing NRPs (D-NRPs) were reported.<sup>17</sup> These D-peptidases could have serious implications for the future of D-NRPs as antibiotics. TriF is a membrane-associated D-peptidase found in the tridecaptin BGC of *Paenibacillus polymyxa* CICC10580 and hydrolyzes the C-terminal side of D-aromatic amino acids. BogQ is a D-peptidase

Received: July 18, 2019

Published: October 28, 2019

that cleaves peptides at the C-terminal side of D-cationic amino acids and is found in the BGC of the bogorols. As ~31% of known D-NRPs contain D-cationic amino acids, BogQ mediated resistance would be problematic. Li et al. identified 403 putative peptidases in the Bacillales order with similar domain compositions to BogQ and found a strong association between these peptidases and NRP BGCs.<sup>17</sup> As the horizontal transfer of entire BGCs is possible, such resistance mechanisms could be transferred to other bacterial species.<sup>18</sup> *In vitro* assays showed BogQ activity toward many D-NRPs, including the tridecaptins, bacitracin, ramoplanin, daptomycin, and a truncated analogue of teixobactin. Both TriF and BogQ rapidly hydrolyze tridecaptin analogues.<sup>11,19</sup> Multiple natural and synthetic tridecaptins have been reported, many of which show strong activity against MDR Gram-negative bacteria and have low toxicity and good serum stability.<sup>19–24</sup> The tridecaptins are also resistant to several major proteases, including trypsin, chymotrypsin, and pepsin.<sup>25</sup> Given the serious problems that D-peptidases could cause for NRP antibiotics, strategies must be found to circumvent their effects. In this study we use the tridecaptins as model substrates to identify chemical modifications that can prevent peptide hydrolysis by TriF and BogQ.

## RESULTS AND DISCUSSION

As part of our group's efforts to identify novel tridecaptin analogues with increased activity against MDR Gram-negative bacteria, we previously synthesized linear (1–8) and cyclic (9–11) variants (Figure 1).<sup>19,20</sup> We showed that cyclization

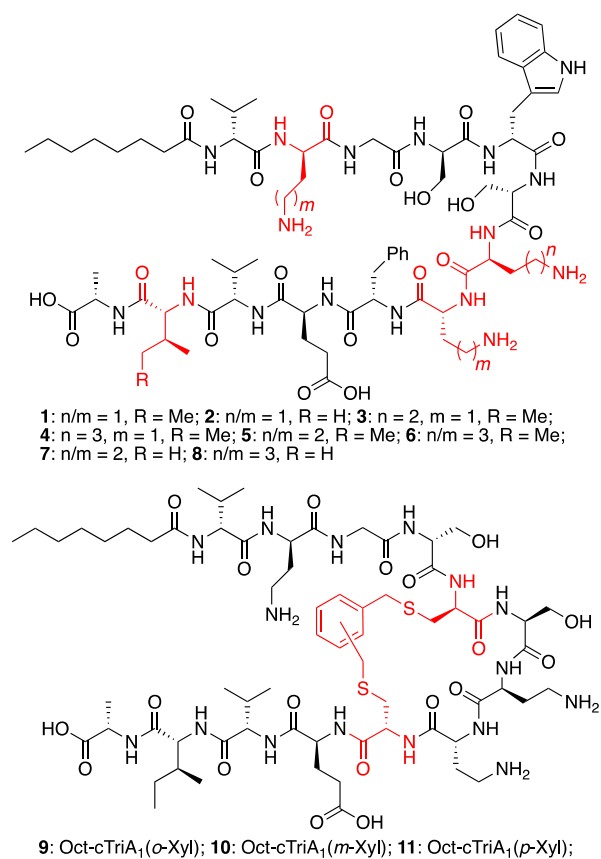


**Figure 1.** Structures of previous reported tridecaptin analogues 1–11. All peptides are susceptible to hydrolysis by BogQ.

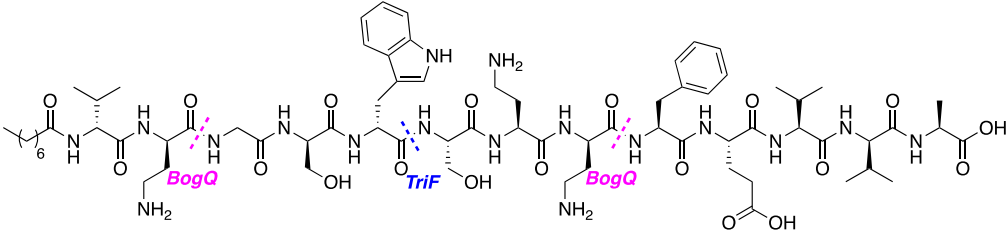
through cross-linking of D-Cys5 and Cys9 with xylene linkers can prevent TriF hydrolysis; however the resulting peptides 9–11 are significantly less active than parent Oct-TriA<sub>1</sub> (1).<sup>19</sup> The BogQ susceptibility of these cyclic tridecaptins was not determined. Linear analogues 3–8 were previously synthesized, where D- and L-Dab residues were replaced with D- and L-Orn/Lys, respectively, to test if conservative substitutions with cheaper amino acids can make tridecaptin synthesis more cost efficient.<sup>20</sup> To determine if any of these modifications were able to impart resistance to BogQ, tridecaptin analogues 1–11 were incubated with this D-peptidase and analyzed by ultraperformance liquid chromatography coupled mass spectrometry (UPLC–MS). We were surprised to find that all analogues are rapidly hydrolyzed by BogQ at the 2 and 8 positions (all >90% after 1 h). This suggests that BogQ is quite promiscuous toward the substrates it accepts, given that it is capable of cleaving D-cationic amino acids with varying chain length, as well as those located within a peptide macrocycle. We therefore considered alternative modifications that could provide D-peptidase resistance.

A number of synthetic modifications can be made to peptides and proteins to improve their stability to peptidases.<sup>26</sup> While we have previously tried cyclization, other strategies such as epimerization at the cleavage site (P) or N-methylation or  $\alpha$ -methylation at the amino acid C-terminal to the cleavage site (P-1) have not been explored with the tridecaptins. We therefore proceeded to synthesize new linear tridecaptins 12–27, where one or more amino acids have been substituted (Table 1). We used derivatives of octyl-tridecaptin A<sub>2</sub> (Oct-TriA<sub>2</sub>) (2) (Val12). Although this peptide is 2- to 4-fold less active than Oct-TriA<sub>1</sub> (1) (D-alle12), it is significantly cheaper to synthesize.<sup>20</sup> The susceptibility of these peptides to BogQ and TriF and their antimicrobial activity against a model Gram-negative (*Escherichia coli* NCTC 12241) and Gram-positive (*Staphylococcus aureus* NCTC 10788) organism were tested (Table 1, Figure 2). Peptides were synthesized from Ala-2-chlorotrityl resin (0.8 mmol/g) using manual or automated (CEM Liberty 12 peptide synthesizer) Fmoc solid-phase peptide synthesis (SPPS).

We first explored modifications that could prevent hydrolysis at D-Dab2 by BogQ. Glycine is the amino acid C-terminal to this cleavage site; therefore we rationalized that placing N-methylglycine (sarcosine, Sar) or 2-aminoisobutyric acid (Aib) at the 3-position would increase steric bulk around this cleavage site, preventing hydrolysis. To test this, Oct-TriA<sub>2</sub>(3-Sar) (12) and Oct-TriA<sub>2</sub>(3-Aib) (13) were synthesized. Unfortunately, these modifications at the 3-position completely abolished antimicrobial activity, with no activity observed against *E. coli* or *S. aureus* at 50  $\mu$ g/mL. Previous studies on the binding mechanism of Oct-TriA<sub>1</sub> to its cellular receptor, the peptidoglycan intermediate lipid II, suggest it encases lipid II on cell membranes through a looped structure.<sup>12</sup> Given that Gly has significantly more rotational freedom than other amino acids, increasing the steric bulk at position 3 likely interferes with the peptides ability to adopt this conformation and bind to lipid II. Replacement of D-Dab2 with L-Dab imparted resistance to BogQ hydrolysis at this site; however the resulting peptide 14 is devoid of antimicrobial activity.

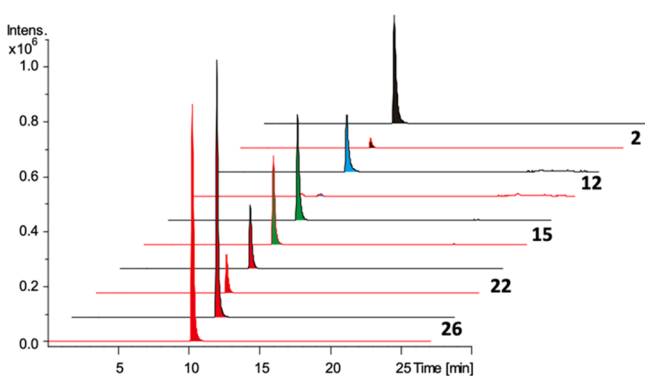
We next proceeded to modify the 9 position in the hope of preventing BogQ hydrolysis at D-Dab8. Peptides containing NMePhe9 or  $\alpha$ MePhe9 were synthesized to test if the increased steric bulk around this position could prevent hydrolysis. Oct-TriA<sub>2</sub>(9-NMePhe) (15) and Oct-TriA<sub>2</sub>(9-

Table 1. D-Peptidase Stability and Antimicrobial Activity of Tridecaptin Analogues 12–27



compd <sup>d</sup>	amino acid modifications <sup>a</sup>							hydrolysis (%) <sup>b</sup>		MIC (μg/mL) <sup>c</sup>	
	AA2	AA3	AA6	AA7	AA8	AA9	AA12	BogQ	TriF <sub>pep</sub>	<i>Ec</i>	<i>Sa</i>
2	D-Dab	Gly	Ser	Dab	D-Dab	Phe	D-Val	>90	100	1.56	50
12	D-Dab	Sar	Ser	Dab	D-Dab	Phe	D-Val	>90		>50	>50
13	D-Dab	Aib	Ser	Dab	D-Dab	Phe	D-Val	>90		>50	>50
14	Dab	Gly	Ser	Dab	D-Dab	Phe	D-Val	60		>50	>50
15	D-Dab	Gly	Ser	Dab	D-Dab	NMePhe	D-Val	15		6.25	>50
16	D-Dab	Gly	Ser	Dab	D-Dab	αMePhe	D-Val	39		>50	>50
17	D-Dab	Sar	Ser	Dab	D-Dab	NMePhe	D-Val	<5		>50	>50
18	D-Dab	Aib	Ser	Dab	D-Dab	NMePhe	D-Val	<5		>50	>50
19	D-Dab	Gly	Ser	Dab	Dab	Phe	D-Val	ND	ND	ND	ND
20	D-Dab	Gly	Sar	Dab	D-Dab	Phe	D-Val	0		3.13	>50
21	D-Dab	Gly	Aib	Dab	D-Dab	Phe	D-Val	0		3.13	>50
22	D-Dab	Gly	Sar	Dab	D-Dab	NMePhe	D-Val	43	0	6.25	>50
23	D-Dab	Gly	Sar	Dab	D-Dab	αMePhe	D-Val	39	0	>50	>50
24	D-Dab	Gly	Sar	Dab	D-Dab	NMePhe	D-Ile	46	0	3.13	>50
25	D-Dab	Gly	Sar	Dab	D-Dab	αMePhe	D-Ile	40	0	>50	>50
26	D-Ala	Gly	Sar	Dab	D-Dab	NMePhe	D-Val	11	0	>50	>50
27	D-Val	Gly	Sar	Dab	D-Dab	NMePhe	D-Val	12	0	>50	>50

<sup>a</sup>Peptides 12–19 were not tested for TriF<sub>pep</sub> resistance as they contain no modification to the TriF cleavage site, and peptides 20 and 21 were not tested for BogQ resistance as they contain no modification to the BogQ cleavage sites. <sup>b</sup>In BogQ and TriF<sub>pep</sub> assays, cleavage ratios in the *in vitro* assay were determined by UPLC–MS, and the reported values represent end-point data after 1 h incubation with BogQ (20 nM) against substrate (50 μM) or after 24 h incubation for TriF<sub>pep</sub> (200 nM). <sup>c</sup>MIC = minimum inhibitory concentration. Determined by microbroth dilutions assays and experiments run in duplicate. Values are shown to three significant figures, and strains used were *E. coli* NCTC 12241 (*Ec*) and *S. aureus* NCTC 10788 (*Sa*). <sup>d</sup>Compound number.



**Figure 2.** Liquid chromatography–mass spectrometry traces of *in vitro* assays of BogQ against Oct-TriA<sub>2</sub> (1, black peaks), Oct-TriA<sub>2</sub>(3-Sar) (12, blue peaks), Oct-TriA<sub>2</sub>(9-NMePhe) (15, green peaks), Oct-TriA<sub>2</sub>(6-Sar, 9-NMePhe) (22, red peaks), and Oct-TriA<sub>2</sub>(2-DAla, 6-Sar, 9-NMePhe) (26, red peaks). Standards (black line) without BogQ and experiments with BogQ (red line) are shown.

αMePhe) (16) are highly resistant to hydrolysis at D-Dab8. The total stability of peptides 15 and 16 to BogQ hydrolysis was also significantly improved, with the NMePhe9 analogue showing only 15% hydrolysis after 1 h incubation and the αMePhe9 analogue showing 39% hydrolysis. In contrast, unmodified Oct-TriA<sub>2</sub> (2) is almost completely hydrolyzed during this time. BogQ is a putative S-layer-associated

peptidase and its S-layer-homology (SLH) domains are rich in negatively charged residues (isoelectric point ~5).<sup>17</sup> The higher activity of BogQ at the 8 position is likely due to increased attraction toward the adjacent Dab7 and D-Dab8 residues. Gratifyingly, Oct-TriA<sub>2</sub>(9-NMePhe) (15) retained strong Gram-negative activity, with a minimum inhibitory concentration (MIC) of 6.25 μg/mL. However, Oct-TriA<sub>2</sub>(9-αMePhe) (16) showed no activity below 50 μg/mL. At the same time, double mutants Oct-TriA<sub>2</sub>(3-Sar, 9-NMePhe) (17) and Oct-TriA<sub>2</sub>(3-Aib, 9-NMePhe) (18) were also synthesized and tested. Although these peptides are highly resistant to BogQ, they are also devoid of antimicrobial activity (MIC > 50 μg/mL). We also synthesized Oct-TriA<sub>2</sub>(Dab8) (19), where the stereochemistry at the 8 position has been inverted. However, the resulting crude peptide proved extremely hydrophobic and we were unable to purify it. D-Dab8 is one of the only essential residues for antimicrobial activity, so it is likely that inverting stereochemistry destroys the peptide's ability to adopt an active secondary structure and leads to a deleterious aggregation.<sup>27</sup>

Having determined that N- or α-methylation of position 9 in the tridecaptins substantially improves resistance to hydrolysis by BogQ, we next tested if modifying the 6 position could overcome TriF hydrolysis at D-Trp5. TriF<sub>pep</sub>, the soluble periplasmic peptidase domain of TriF, was used in these assays. A previous alanine scan of Oct-TriA<sub>1</sub> found that substitution of Ser6 had minimal effect of antimicrobial activity;<sup>27</sup> therefore

we rationalized that incorporating N- or  $\alpha$ -methylated amino acids at this position could impart resistance to TriF. Oct-TriA<sub>2</sub>(6-Sar) (**20**) and Oct-TriA<sub>2</sub>(6-Aib) (**21**) were synthesized and found to be completely resistant to TriF and retain strong activity (3.13  $\mu\text{g}/\text{mL}$ ) against *E. coli*. Although we have previously synthesized cyclic tridecaptin analogues that are resistant to TriF, these peptides were significantly less active than their linear counterparts. Discovering that a simple substitution of Ser6 with Sar or Aib provides complete TriF resistance with negligible loss in activity is a welcome development.

With optimal single modifications for improving stability toward BogQ and TriF identified, we next attempted to generate tridecaptin analogues that are resistant to both D-peptidases. Oct-TriA<sub>2</sub>(6-Sar, 9-NMePhe) (**22**) and Oct-TriA<sub>2</sub>(6-Sar, 9- $\alpha$ MePhe) (**23**) are both resistant to TriF and are significantly more stable toward BogQ hydrolysis than the unmodified peptide. Importantly, Oct-TriA<sub>2</sub>(6-Sar, 9-NMePhe) (**22**) also retains strong activity against *E. coli* (6.25  $\mu\text{g}/\text{mL}$ ). A previous tridecaptin SAR study found that having D-*allo*-Ile at the 12 position (as in Oct-TriA<sub>1</sub>) provides a 2- to 4-fold increase in antimicrobial activity.<sup>20</sup> Therefore, Oct-TriA<sub>1</sub> analogues **24** and **25**, which incorporate some of these modifications, were synthesized and tested. As expected, peptides **24** and **25** have total TriF resistance and substantially improved BogQ resistance; however substitution of D-Val12 with D-*allo*-Ile had minimal effect on antimicrobial activity. It was previously reported that substitution of D-Dab2 with D-Ala is tolerated, although the resulting peptide is 2- to 4-fold less active. In a final effort to identify new active tridecaptins with enhanced stability at all three D-peptidase cleavage sites, peptides **26** and **27**, wherein D-Dab2 has been substituted with D-Ala and D-Val, respectively, were synthesized. Both analogues have excellent stability toward BogQ and TriF; however their antimicrobial activities are diminished, with MIC of >50  $\mu\text{g}/\text{mL}$  against *E. coli*.

We next tested the activity of Oct-TriA<sub>2</sub> (**2**) and peptides **15**, **20**, **22**, and **26** against sheep erythrocytes, each at 100  $\mu\text{g}/\text{mL}$  for 30 min. This is >30 times that required for total bactericidal activity. At 100  $\mu\text{g}/\text{mL}$ , Oct-TriA<sub>2</sub> (**2**) caused 53% lysis, whereas peptides **15**, **20**, and **22** show levels of hydrolysis at 30%, 38%, and 60%, respectively. In contrast, peptide **22** was more hemolytic than Oct-TriA<sub>2</sub> (**2**), causing 78% hydrolysis. These results are promising and show that hemolytic activity is not significant for most of these new tridecaptin analogues.

Having identified lead tridecaptin analogues with improved D-peptidase stability, we next proceeded to study their mechanism of action. Tridecaptin A<sub>1</sub> kills Gram-negative bacteria through a receptor-mediated membrane-lysis mechanism, whereby it binds to lipid II on the surface of the inner membrane and disrupts the proton motive force.<sup>12</sup> As amphiphilic peptides like the tridecaptins can also kill bacteria through a nonspecific detergent-like effect, we sought to determine whether these novel tridecaptin analogues could still bind to lipid II. Previous studies showed that TriA<sub>1</sub> binds to both Gram-positive and Gram-negative lipid II, although it has a much higher affinity for the Gram-negative analogue. To assay if these novel tridecaptin analogues can still bind to lipid II, we performed *in vitro* lipid II-binding assays, which are an effective way to determine if peptides bind to lipid II using spot-on-lawn assays (Figure 3).<sup>12</sup> Given the qualitative nature of these experiments, we chose to use Gram-positive lipid II, which we previously prepared by total chemical synthesis.<sup>28</sup>

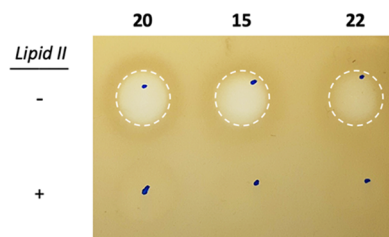


**Figure 3.** Spot-on-lawn-assay with *E. coli* NCTC 12241 used to show lipid II binding of tridecaptin analogues **15**, **20**, and **22**. Peptide solutions (10  $\mu\text{L}$ , 60  $\mu\text{M}$ ) are spotted onto a MH Agar plate freshly impregnated with *E. coli*, and the resulting plate is incubated at 37  $^{\circ}\text{C}$  for 16 h. In the top lane, a zone of inhibition for all peptides signifies their antimicrobial activity. In the bottom lane, no zone of inhibition is observed for peptides that have been premixed with excess lipid II, which sequesters peptides by complex formation.

Oct-TriA<sub>2</sub>(9-NMePhe) (**15**), Oct-TriA<sub>2</sub>(6-Sar) (**20**), and Oct-TriA<sub>2</sub>(6-Sar, 9-NMePhe) (**22**) were incubated with an excess (7 equiv) of lipid II for 30 min, before being applied to a freshly prepared agar plate that had been inoculated with *E. coli* and incubated for 18 h at 37  $^{\circ}\text{C}$ . Whereas a clear zone of inhibition was observed for each peptide when no lipid II is present, the addition of lipid II sequesters antimicrobial activity, showing that synthetic tridecaptin analogues **15**, **20**, and **22** retain lipid II binding. Coupled with their comparable antimicrobial activity to Oct-TriA<sub>1</sub>, these results suggest these analogues kill Gram-negative bacteria through the same mechanism as the natural peptide.

## CONCLUSION

Nonribosomal peptides have been an essential source of antibiotics; however, the emergence of D-peptidases could pose a major problem for their continued use. It is therefore imperative that we develop strategies against them. In this study we identified several synthetic modifications that impart resistance to the D-peptidases TriF and BogQ. New synthetic tridecaptin analogues were synthesized that retain strong antimicrobial activity and are significantly more stable to hydrolysis by these D-peptidases. These modifications do not interfere with mechanism of action, which was corroborated using *in vitro* lipid II binding ability assays.

## EXPERIMENTAL SECTION

**General.** All proteinogenic Fmoc-amino acids used in this study were purchased from CEM. The remaining Fmoc-amino acids, HATU, TFA and TIPS were purchased from Fluorochem. Ala-2-chlorotrityl resin and DIPEA were purchased from Sigma-Aldrich. HPLC grade ACN, DCM, and DMF were purchased from Merck. All chemicals were used without further purification. Peptide purity was determined by analytical HPLC and in all instances found to be >95%.

**Peptide Synthesis.** Peptides **1–11** were synthesized and purified as previously described.<sup>19,20</sup> Peptides **12–27** were synthesized automatically using a CEM Liberty 12 microwave peptide synthesizer or manually in a Merrifield vessel. Automated SPPS was performed on a 0.1 mmol scale using Fmoc chemistry on 2CT resin preloaded with alanine (0.8 mmol/g). Factory settings were used for all coupling and deprotection cycles. Asymmetrically protected amino acids were used as 0.2 M solutions in DMF, with amino acid subunits being coupled using HATU as the activator and DIPEA as the activator base and heated to 70  $^{\circ}\text{C}$  for 5 min. Fmoc residues were deprotected using a 20% solution of piperidine in DMF. An initial deprotection was performed at 70  $^{\circ}\text{C}$  for 0.5 min, followed by an additional deprotection at 70  $^{\circ}\text{C}$  for 3 min. Manual SPPS was also performed

on a 0.1 mmol scale using Fmoc chemistry on 2CT resin preloaded with alanine (0.8 mmol/g). Reactions were performed in a 20 mL glass fritted column fitted with a T-joint and three-way T-bore PTFE stopcock. Resin was preswollen by bubbling in DMF (5 mL, 10 min) with argon. Between deprotections and couplings the vessel was drained under argon pressure and washed with DMF (3 × 5 mL). The Fmoc group was removed by bubbling with 20% piperidine in DMF (3 × 5 mL × 1 min). The desired amino acid (5 equiv) was preactivated by shaking with HATU (5 equiv) and DIPEA (10 equiv) in DMF (5 mL) for 5 min. The resin was bubbled in the coupling solution for 1 h, drained, and washed with DMF (3 × 5 mL). Deprotection and coupling steps were continued to complete the peptide synthesis. Upon completion of synthesis, the peptide resin was washed with DCM (3 × 5 mL) and dried under vacuum suction for 15 min. Global deprotection and resin cleavage was performed using TFA/TIPS/H<sub>2</sub>O (95:2.5:2.5, 10 mL) at 37 °C for 1 h, with periodic shaking. The solution was filtered through glass wool and concentrated *in vacuo*. Et<sub>2</sub>O was added, the suspension centrifuged (3500 rpm, 3 min), and solvent decanted off. The resulting crude peptide was diluted in a minimal volume of 1:4 ACN/H<sub>2</sub>O 0.1% TFA solution for purification.

**Purification and Analysis of Peptides.** Peptides were purified by RP-HPLC using a Phenomenex Luna C18 column (5 μm, 250 mm × 21.2 mm) with a 2 mL sample loop. ThermoFisher Chromeleon 7.2 software was used to operate the PerkinElmer 200 series HPLC system. Flow rate was set at 10 mL/min, and the UV/vis detector was set to measuring at 220 nm. Gradient elution was employed with 0.1% TFA in Milli-Q H<sub>2</sub>O (A) and 0.1% TFA in ACN (B). Starting from 20% B and 80% A for 5 min, B was ramped up to 55% over 30 min and then to 95% over 3 min. The method stayed at 95% B for 3 min before ramping down to 20% B over 2 min and being held for 5 min. Product containing fractions were pooled, concentrated *in vacuo*, frozen, and lyophilized to remove water and yield products typically as white flocculent solids. Peptide purity was quantified by analytical HPLC. A Phenomenex Luna C18 column (5 μm, 150 mm × 4.6 mm) was used, with samples injected onto a 200 μL sample loop. The flow rate was set at 2 mL/min and UV/vis absorbance measured at 220 nm. Gradient elution was again employed using the same solvents A and B. It began at 20% B and 80% A for 2 min before ramping to 95% B over 18 min. B was then decreased to 20% over 0.1 min and held for 3.9 min. Electrospray ionization high resolution mass spectrometry (ESI-HRMS) was carried out on all purified peptides using a Waters LCT Premier ToF mass spectrometer.

**Oct-TriA<sub>2</sub> (3-Sar) (12).** >95% purity, 17.2 mg, 11.3%. HRMS (ESI) calcd for C<sub>72</sub>H<sub>113</sub>N<sub>17</sub>O<sub>19</sub> [M - H]<sup>-</sup> 1518.8326, found 1518.8326.

**Oct-TriA<sub>2</sub> (3-Aib) (13).** >95% purity, 13.4 mg, 8.7%. HRMS (ESI) calcd for C<sub>73</sub>H<sub>115</sub>N<sub>17</sub>O<sub>19</sub> [M + H]<sup>+</sup> 1534.8626, found 1534.8575.

**Oct-TriA<sub>2</sub> (2-Dab) (14).** >95% purity, 45.2 mg, 30.0%. HRMS (ESI) calcd for C<sub>71</sub>H<sub>111</sub>N<sub>17</sub>O<sub>19</sub> [M - H]<sup>-</sup> 1504.8169, found 1504.8191.

**Oct-TriA<sub>2</sub> (9-NMePhe) (15).** >95% purity, 15.1 mg, 9.9%. HRMS (ESI) calcd for C<sub>72</sub>H<sub>113</sub>N<sub>17</sub>O<sub>19</sub> [M + H]<sup>+</sup> 1520.8472, found 1520.8451.

**Oct-TriA<sub>2</sub> (9-αMePhe) (16).** >95% purity, 32.4 mg, 21.3%. HRMS (ESI) calcd for C<sub>72</sub>H<sub>113</sub>N<sub>17</sub>O<sub>19</sub> [M - H]<sup>-</sup> 1518.8326, found 1518.8320.

**Oct-TriA<sub>2</sub> (3-Sar, 9-NMePhe) (17).** >95% purity, 14.8 mg, 9.6%. HRMS (ESI) calcd for C<sub>73</sub>H<sub>115</sub>N<sub>17</sub>O<sub>19</sub> [M + H]<sup>+</sup> 1534.8626, found 1534.8619.

**Oct-TriA<sub>2</sub> (3-Aib, 9-NMePhe) (18).** >95% purity, 7.9 mg, 5.1%. HRMS (ESI) calcd for C<sub>74</sub>H<sub>117</sub>N<sub>17</sub>O<sub>19</sub> [M + 2H]<sup>2+</sup> 774.9429, found 774.9439.

**Oct-TriA<sub>2</sub> (8-Dab) (19).** Peptide aggregation prevented purification; therefore activity and peptidase stability could not be tested.

**Oct-TriA<sub>2</sub> (6-Sar) (20).** >95% purity, 6.1 mg, 4.1%. HRMS (ESI) calcd for C<sub>71</sub>H<sub>111</sub>N<sub>17</sub>O<sub>18</sub> [M + 2H]<sup>2+</sup> 745.9219, found 745.9250.

**Oct-TriA<sub>2</sub> (6-Aib) (21).** >95% purity, 5.7 mg, 3.8%. HRMS (ESI) calcd for C<sub>72</sub>H<sub>113</sub>N<sub>17</sub>O<sub>18</sub> [M + H]<sup>+</sup> 1504.8522, found 1504.8524.

**Oct-TriA<sub>2</sub> (6-Sar, 9-NMePhe) (22).** >95% purity, 17.7 mg, 11.8%. HRMS (ESI) calcd for C<sub>72</sub>H<sub>113</sub>N<sub>17</sub>O<sub>18</sub> [M + H]<sup>+</sup> 1504.8522, found 1504.8615.

**Oct-TriA<sub>2</sub> (6-Sar, 9-αMePhe) (23).** >95% purity, 9.3 mg, 6.2%. HRMS (ESI) calcd for C<sub>72</sub>H<sub>113</sub>N<sub>17</sub>O<sub>18</sub> [M + H]<sup>+</sup> 1504.8522, found 1504.8577.

**Oct-TriA<sub>1</sub> (6-Sar, 9-NMePhe) (24).** >95% purity, 12.6 mg, 8.3%. HRMS (ESI) calcd for C<sub>73</sub>H<sub>115</sub>N<sub>17</sub>O<sub>18</sub> [M + 2H]<sup>2+</sup> 759.9376, found 759.9428.

**Oct-TriA<sub>2</sub> (6-Sar, 9-αMePhe) (25).** >95% purity, 11.2 mg, 7.4%. HRMS (ESI) calcd for C<sub>73</sub>H<sub>115</sub>N<sub>17</sub>O<sub>18</sub> [M + 2H]<sup>2+</sup> 759.9376, found 759.9392.

**Oct-TriA<sub>2</sub> (2-DAla, 6-Sar, 9-NMePhe) (26).** >95% purity, 49.9 mg, 33.8%. HRMS (ESI) calcd for C<sub>71</sub>H<sub>110</sub>N<sub>16</sub>O<sub>18</sub> [M + 2H]<sup>2+</sup> 738.4165, found 738.4145.

**Oct-TriA<sub>2</sub> (2-DVal, 6-Sar, 9-NMePhe) (27).** >95% purity, 39.1 mg, 26.0%. HRMS (ESI) calcd for C<sub>73</sub>H<sub>114</sub>N<sub>16</sub>O<sub>18</sub> [M + 2H]<sup>2+</sup> 752.4321, found 752.4620.

**Antimicrobial Testing.** Minimum inhibitory concentrations (MICs) were determined according to Clinical and Standards Laboratory Institute (CLSI) guidelines. Briefly, peptides were dissolved in Muller–Hinton broth (MHB) and serial dilutions made across a 96-well plate. Each well was inoculated with a suspension of the required bacterial strain to reach a final inoculum of 5 × 10<sup>5</sup> colony forming units per mL. The MIC was taken as the lowest concentration with no visible (cloudy suspension) growth after 18 h. The antimicrobial activity of each peptide was determined in duplicate in three independent experiments and found to be consistent across all experiments.

**Peptide Hydrolysis Assays with BogQ and TriF<sub>pep</sub>.** For expression of D-peptidases, the recombinant strain *E. coli* BL21 carrying pET-28a-bogQ or pET-24a-triF<sub>pep</sub> was cultured overnight at 37 °C in LB medium. This was diluted 1:100 into 100 mL of LB medium containing 50 μg/mL kanamycin and incubated at 37 °C until OD<sub>600</sub> = 0.4–0.6 was reached. The culture was incubated at 15 °C for 30 min, and isopropyl β-D-1-thiogalactopyranoside was added to a final concentration of 200 μM.<sup>17</sup> The target proteins purified using Ni-NTA purification. The assay mixture (total volume 30 μL in 25% PBS buffer, pH 7.4), containing purified protein (BogQ, 20 nM or TriF<sub>pep</sub> 200 nM) and synthetic analogues (50 μM), was incubated for 1 h (BogQ) or 24 h (TriF<sub>pep</sub>) at 37 °C. Reactions were quenched with three volumes of cold methanol (90 μL) and centrifuged at 15 000 rpm for 10 min to precipitate protein. The supernatant (2 μL) was subjected to UPLC–MS analysis for the determination of cleavage ratios.<sup>17</sup> Assays were repeated in two independent experiments and results consistent across both.

**Hemolytic Assays.** A 96-well plate containing PBS solutions (100 μL) of tridecaptin analogues **2**, **15**, **20**, **22**, and **26** (200 μg/mL) (experiments run in triplicate) was prepared. 0.1% Triton X-100 (100 μL) was used as a positive control, while PBS (100 μL) was used as a blank. Defibrinated sheep blood (0.5 mL) was diluted with phosphate-buffered saline (9.5 mL), gently shaken, and centrifuged (5600 rpm, 5 min). This process was repeated three more times to remove any free hemoglobin. The resulting erythrocyte pellet was gently resuspended in 9.5 mL of PBS. Aliquots of the resulting mixture (100 μL) were added to the appropriate wells on the 96-well plate, and the plate was incubated at 37 °C for 30 min. The samples were then gently mixed by pipetting, and 20 μL of each was added to 200 μL of PBS. Once again, the samples were gently mixed. The diluted samples were then centrifuged (7000 rpm, 5 min), and supernatant (150 μL) from each sample was added to a new 96-well plate. The absorbance of each sample was individually measured at 415 nm using a Denovix DS-11 FX+ spectrophotometer. Percent hemolysis of the peptides was calculated relative to Triton X-100. Assays were repeated in two independent experiments and results consistent, and % hemolysis was taken as the average of these values.

**Lipid II Binding Assays.** The ability of selected peptides **15**, **20**, and **22** to bind to lipid II was assessed using a previously published peptide sequestration assay.<sup>12</sup> *E. coli* impregnated agar plates were prepared as follows: Morphologically similar colonies of *E. coli* NCTC

12241 were suspended in MHB (100  $\mu\text{L}$ ) to a density of  $\text{OD}_{600} \sim 1.0$ . The resulting suspension (100  $\mu\text{L}$ ) was used to inoculate molten (37  $^{\circ}\text{C}$ ) Mueller–Hinton agar (MHA) (0.75% agarose) (10 mL). This mixture was immediately poured on top of MHA (1.5% agarose) and allowed to solidify. The minimum concentration of each peptide required for a clear zone of inhibition was determined by spotting different concentrations of each peptide (each 10  $\mu\text{L}$ ) and incubating plates for 16 h at 37  $^{\circ}\text{C}$ . For peptides 15, 20, and 22 the optimal concentration was 60  $\mu\text{M}$ . The lipid II used in these assays was chemically synthesized as previously described.<sup>28</sup> 1:7 solutions of peptide:Gram-positive lipid II (total volume 10  $\mu\text{L}$ ), in which the final concentration of peptide is 60  $\mu\text{M}$ , were prepared from solutions of each peptide (1 mg/mL), lipid II (2 mg/mL), and Milli-Q  $\text{H}_2\text{O}$ . Solutions were incubated at 37  $^{\circ}\text{C}$  before being spotted onto *E. coli* impregnated agar plates. 60  $\mu\text{M}$  solutions of peptides without lipid II were also spotted, and the resulting plate was incubated for 16 h at 37  $^{\circ}\text{C}$ . Lipid II sequestration of peptides is visualized by the inhibition of antimicrobial activity. Results were consistent across two independent experiments.

## ■ ASSOCIATED CONTENT

### Supporting Information

The Supporting Information is available free of charge on the ACS Publications website at DOI: 10.1021/acs.jmedchem.9b01078.

Compound characterization and details of *in vitro* assays (PDF)

## ■ AUTHOR INFORMATION

### Corresponding Author

\*E-mail: s.cochrane@qub.ac.uk.

### ORCID

Stephen A. Cochrane: 0000-0002-6239-6915

### Author Contributions

S.J.B., R.D.B., and C.E.M. did peptide synthesis and antimicrobial assays. Y.-X.L. did peptidase assays. S.A.C. prepared the manuscript. All authors have given approval to the final version of the manuscript.

### Notes

The authors declare no competing financial interest.

## ■ ACKNOWLEDGMENTS

We thank Conor McGrann and Darren Baskerville for assistance with mass spectrometry, Panagiotis Manesiotis for assistance with HPLC, and Chris Lohans for advice during manuscript preparation. We acknowledge financial support from the Wellcome Trust (Grant 110270/A/15/Z, S.A.C.), Queen's University Belfast (start-up grant, S.A.C.) and the Hong Kong Branch of Southern Marine Science and Engineering Guangdong Laboratory (SMSEGL20SC01, Y.-X.L. & P.-Y.Q.).

## ■ ABBREVIATIONS USED

ACN, acetonitrile; BGC, biosynthetic gene cluster; 2-CT, 2-chlorotrityl; DCM, dichloromethane; DIPEA, diisopropylethylamine; DMF, dimethylformamide; Fmoc, fluorenylmethoxycarbonyl; HATU, *O*-(7-azabenzotriazol-1-yl)-*N,N,N',N'*-tetramethyluronium hexafluorophosphate; HPLC, high-performance liquid chromatography; MDR, multidrug resistant; MIC, minimum inhibitory concentration; NCTC, National Culture and Tissue Collection; NRP, nonribosomal peptide; NRPS, nonribosomal peptide synthetase; Oct, octanoyl; SLH, S-layer homology; SPPS, solid-phase peptide synthesis; TFA,

trifluoroacetic acid; Tri, tridecaptin; UPLC–MS, ultra-performance liquid–chromatography coupled mass spectrometry

## ■ REFERENCES

- (1) Süssmuth, R. D.; Mainz, A. Nonribosomal peptide synthesis—principles and prospects. *Angew. Chem., Int. Ed.* **2017**, *56*, 3770–3821.
- (2) Winn, M.; Fyans, J. K.; Zhuo, Y.; Micklefield, J. Recent advances in engineering nonribosomal peptide assembly lines. *Nat. Prod. Rep.* **2016**, *33*, 317–347.
- (3) Böttger, R.; Hoffmann, R.; Knappe, D. Differential stability of therapeutic peptides with different proteolytic cleavage sites in blood, plasma and serum. *PLoS One* **2017**, *12*, e0178943.
- (4) Brown, E. D.; Wright, G. D. Antibacterial drug discovery in the resistance era. *Nature* **2016**, *529*, 336–343.
- (5) Harvey, A. L.; Edrada-Ebel, R.; Quinn, R. J. The re-emergence of natural products for drug discovery in the genomics era. *Nat. Rev. Drug Discovery* **2015**, *14*, 111–129.
- (6) Liu, Y.; Ding, S.; Shen, J.; Zhu, K. Nonribosomal antibacterial peptides that target multidrug-resistant bacteria. *Nat. Prod. Rep.* **2019**, *36*, 573–592.
- (7) Ling, L. L.; Schneider, T.; Peoples, A. J.; Spoering, A. L.; Engels, I.; Conlon, B. P.; Mueller, A.; Schäberle, T. F.; Hughes, D. E.; Epstein, S.; Jones, M.; Lazarides, L.; Steadman, V. A.; Cohen, D. R.; Felix, C. R.; Fetterman, K. A.; Millett, W. P.; Nitti, A. G.; Zullo, A. M.; Chen, C.; Lewis, K. A new antibiotic kills pathogens without detectable resistance. *Nature* **2015**, *517*, 455–459.
- (8) Zipperer, A.; Konnerth, M. C.; Laux, C.; Berscheid, A.; Janek, D.; Weidenmaier, C.; Burian, M.; Schilling, N. A.; Slavetinsky, C.; Marschal, M.; Willmann, M.; Kalbacher, H.; Schitteck, B.; Brötz-Oosterhelt, H.; Grond, S.; Peschel, A.; Krismer, B. Human commensals producing a novel antibiotic impair pathogen colonization. *Nature* **2016**, *535*, 511–516.
- (9) Hamamoto, H.; Urai, M.; Ishii, K.; Yasukawa, J.; Paudel, A.; Murai, M.; Kaji, T.; Kuranaga, T.; Hamase, K.; Katsu, T.; Su, J.; Adachi, T.; Uchida, R.; Tomoda, H.; Yamada, M.; Souma, M.; Kurihara, H.; Inoue, M.; Sekimizu, K. Lysocin E is a new antibiotic that targets menaquinone in the bacterial membrane. *Nat. Chem. Biol.* **2015**, *11*, 127–133.
- (10) Chu, J.; Vila-Farres, X.; Inoyama, D.; Ternei, M.; Cohen, L. J.; Gordon, E. A.; Reddy, B. V.; Charlop-Powers, Z.; Zebroski, H. A.; Gallardo-Macias, R.; Jaskowski, M.; Satish, S.; Park, S.; Perlin, D. S.; Freundlich, J. S.; Brady, S. F. Discovery of MRSA active antibiotics using primary sequence from the human microbiome. *Nat. Chem. Biol.* **2016**, *12*, 1004–1006.
- (11) Li, Y. X.; Zhong, Z.; Zhang, W. P.; Qian, P. Y. Discovery of cationic nonribosomal peptides as Gram-negative antibiotics through global genome mining. *Nat. Commun.* **2018**, *9*, 3273.
- (12) Cochrane, S. A.; Findlay, B.; Bakhtiyari, A.; Acedo, J. Z.; Rodriguez-Lopez, E. M.; Mercier, P.; Vederas, J. C. Antimicrobial lipopeptide tridecaptin A1 selectively binds to Gram-negative lipid II. *Proc. Natl. Acad. Sci. U. S. A.* **2016**, *113*, 11561–11566.
- (13) Johnston, C. W.; Skinnider, M. A.; Dejong, C. A.; Rees, P. N.; Chen, G. M.; Walker, C. G.; French, S.; Brown, E. D.; Bérdy, J.; Liu, D. Y.; Magarvey, N. A. Assembly and clustering of natural antibiotics guides target identification. *Nat. Chem. Biol.* **2016**, *12*, 233–239.
- (14) Forsberg, K. J.; Reyes, A.; Wang, B.; Selleck, E. M.; Sommer, M. O.; Dantas, G. The shared antibiotic resistome of soil bacteria and human pathogens. *Science* **2012**, *337*, 1107–1111.
- (15) Jiang, X.; Ellabaan, M. M. H.; Charusanti, P.; Munck, C.; Blin, K.; Tong, Y.; Weber, T.; Sommer, M. O. A.; Lee, S. Y. Dissemination of antibiotic resistance genes from antibiotic producers to pathogens. *Nat. Commun.* **2017**, *8*, 15784.
- (16) Thaker, M. N.; Wang, W.; Spanogiannopoulos, P.; Waglechner, N.; King, A. M.; Medina, R.; Wright, G. D. Identifying producers of antibacterial compounds by screening for antibiotic resistance. *Nat. Biotechnol.* **2013**, *31*, 922–927.
- (17) Li, Y. X.; Zhong, Z.; Hou, P.; Zhang, W. P.; Qian, P. Y. Resistance to nonribosomal peptide antibiotics mediated by D-stereospecific peptidases. *Nat. Chem. Biol.* **2018**, *14*, 381–387.

(18) Moffitt, M. C.; Neilan, B. A. Characterization of the nodularin synthetase gene cluster and proposed theory of the evolution of cyanobacterial hepatotoxins. *Appl. Environ. Microbiol.* **2004**, *70*, 6353–6362.

(19) Ballantine, R. D.; Li, Y. X.; Qian, P. Y.; Cochrane, S. A. Rational design of new cyclic analogues of the antimicrobial lipopeptide tridecaptin A<sub>1</sub>. *Chem. Commun.* **2018**, *54*, 10634–10637.

(20) Ballantine, R. D.; McCallion, C. E.; Nassour, E.; Tokajian, S.; Cochrane, S. A. Tridecaptin-inspired antimicrobial peptides with activity against multidrug-resistant Gram-negative bacteria. *MedChemComm* **2019**, *10*, 484–487.

(21) Cochrane, S. A.; Lohans, C. T.; Brandelli, J. R.; Mulvey, G.; Armstrong, G. D.; Vederas, J. C. Synthesis and structure-activity relationship studies of N-terminal analogues of the antimicrobial peptide tridecaptin A<sub>1</sub>. *J. Med. Chem.* **2014**, *57*, 1127–1131.

(22) Cochrane, S. A.; Vederas, J. C. Unacylated tridecaptin A<sub>1</sub> acts as an effective sensitizer of Gram-negative bacteria to other antibiotics. *Int. J. Antimicrob. Agents* **2014**, *44*, 493–499.

(23) Cochrane, S. A.; Lohans, C. T.; van Belkum, M. J.; Bels, M. A.; Vederas, J. C. Studies on tridecaptin B<sub>1</sub>, a lipopeptide with activity against multidrug resistant Gram-negative bacteria. *Org. Biomol. Chem.* **2015**, *13*, 6073–6081.

(24) Cochrane, S. A.; Li, X.; He, S.; Yu, M.; Wu, M.; Vederas, J. C. Synthesis of tridecaptin–antibiotic conjugates with in vivo activity against Gram-negative bacteria. *J. Med. Chem.* **2015**, *58*, 9779–9785.

(25) Cochrane, S. A. Structural and Mechanistic Studies on Antimicrobial Lipopeptides. Ph.D. Thesis, University of Alberta, 2016.

(26) McKinnie, S. M. K.; Wang, W.; Fischer, C.; McDonald, T.; Kalin, K. R.; Iturrioz, X.; Llorens-Cortes, C.; Oudit, G. Y.; Vederas, J. C. Synthetic modification within the “RPRL” region of apelin peptides: Impact on cardiovascular activity and stability to neprilysin and plasma degradation. *J. Med. Chem.* **2017**, *60*, 6408–6427.

(27) Cochrane, S. A.; Findlay, B.; Vederas, J. C.; Ratemi, E. S. Key residues in octyl-tridecaptin A<sub>1</sub> analogues linked to stable secondary structures in the membrane. *ChemBioChem* **2014**, *15*, 1295–1299.

(28) Dong, Y. Y.; Wang, H.; Pike, A. C. W.; Cochrane, S. A.; Hamedzadeh, S.; Wyszynski, F. J.; Bushell, S. R.; Royer, S. F.; Widdick, D. A.; Sajid, A.; Boshoff, H. I.; Park, Y.; Lucas, R.; Liu, W. M.; Lee, S. S.; Machida, T.; Minall, L.; Mehmood, S.; Belaya, K.; Liu, W. W.; Chu, A.; Shrestha, L.; Mukhopadhyay, S. M. M.; Strain-Damerell, C.; Chalk, R.; Burgess-Brown, N. A.; Bibb, M. J.; Barry, C. E., III; Robinson, C. V.; Beeson, D.; Davis, B. G.; Carpenter, E. P. Structures of DPAGT1 explain glycosylation disease mechanisms and advance TB antibiotic design. *Cell* **2018**, *175*, 1045–1058.